


Second Order Dispersion In The Interferometer's Optical Elements For Quantum Cryptography (QC) System

Duha S. Ahmed  Ahlam L. huraiji**, Ali K. Abdul-Fattah*** & Adawiya J. Haider***

Received on: 15/6/2008

Accepted on: 9/10/2008

Abstract

In this study, we have studied the entangled photon source and how the coincident count rate and visibility could be affected by the optical elements of the system setup. The profile of the interference dip of the optical elements for Quantum Cryptography (QC) system is modified by the increase of the second order dispersion parameter (D_p) and lead to increase of visibility. Non zero chirp parameter (a_i) of the pump beam can provide a higher central peak but on the other hand it reduces the visibility, the peak remains, while the dispersion in an optical element through which down converted photon propagate leads to asymmetry in the interference pattern dip, the dip is particularly stretched with larger value of birefringent material length (20-30)mm. The highest visibility at birefringent material dispersion (d) equals to zero, and the dip was broader at larger value of (d).

Keywords: quantum cryptography (QC); entangled photons, laser.

الخلاصة

تم في هذا العمل دراسة قابلية الرؤية كدالة لتأخير المسار البصري، وقد أظهرت النتائج ان شكل منخفض التداخل يتغير بزيادة معلمة التشتت من الدرجة الثانية (D_p) وبالتالي زيادة قابلية الرؤية إن معلمة الزقزقة اللاصفريية (a_i) لنبضة الضخ تعطي قمم متمركزة عالية ومن ناحية تؤدي الى انخفاض قابلية الرؤية، وعند البلورات الطويلة تبقى القمم ثابتة بينما يؤدي التشتت في العناصر البصرية الى التشوه في منخفض نمط التداخل وتتوسع المنخفضات عند الأطوال الكبيرة للمادة ثنائية الانكسار ($l= 20-30\text{mm}$) وأعلى رؤيا عند عندما يكون تشتت المواد ثنائية الانكسار ($d=0$) فيما يكون المنخفض أكثر عرضا.

* Applied Science Department, University of Technology/ Baghdad

** College of Science, University of Baghdad/ Baghdad

*** Applied Science Department, University of Technology/ Baghdad

1-Introduction

Dispersion plays an important role in the propagation of short classical optical pulses and of quantum wave packets. In particular, transform-limited classical pulses as well as single-photon wave packets experience temporal broadening upon propagating through a dispersive medium.

In classical applications such as communication over optical fibers this pulse broadening ultimately limits the data transfer rates, unless appropriate compensation methods are implemented. In the case of quantum communications over fibers, the data rates are sufficiently low that such considerations are not necessary. Nonetheless, the presence of dispersive systems in the path between source and detector can compromise certain important quantum phenomena that are central to some of the communications protocols, such as teleportation and dense coding, which rely on entangled photon multiples [1,2].

As for any classical communication system, in quantum cryptography systems we have to achieve high bit rates for long distances with minimum QBER for the secure transmitted data.

Until now the photons are the basic quantum system used for quantum communication systems. Using photons in these systems present a problem of losing the photon in the quantum channel by which the transmission distance will be limited to the order of 170 km, with the present day silica fiber and selectors [3].

All quantum cryptographic systems suffer from two main problems. For polarization based encoding systems, the polarization must be kept constant over tens of kilometers, while in interferometric systems, which are generally based on two unbalanced Mach-Zehnder interferometers. They must be adjusted with respect to each other every few seconds to compensate for thermal drifts. The other essential problem is

the high noise of photon counters that leads to an increase in QBER.

Regarding photon source, experiments and theory studies are directed towards improvement at photon sources to produce real single photon sources to avoid eavesdropping and to increase security and reduce QBER [5,4].

2. Theoretical Analysis

2.1 Second-Order Dispersion for Entangled Photon

In this work a theoretical investigation of dispersion effects in femtosecond-pulsed SPDC is devoted. Particular attention is given to the effects of pump pulse chirp and second orders dispersion (in both the pump and down-converted beams) invisibility and shape of the photo-coincidence pattern. Dispersion cancellation which has been extensively studied in the case CW pumping is also predicted to occur under certain conditions for femtosecond down converted down converted pairs. We consider a non linear crystal pumped by a strong coherent-state field. Non-linear interaction then leads to the spontaneous parametric down conversion. The two photon amplitude A_{12} depends only on the differences t_1-t and t_2-t , When the down converted beams propagate through a dispersive material of the length l , the entangled two photon state $1\psi^{(2)}\rangle$ [6,7].

The proposal set up for coincidence-count measurement is shown in Fig. (1). The consider type- II parametric down conversion for this work, using a beam splitter 50/50 and the polarized photons are detected at the detectors D_A and D_B .

In this case two mutually perpendicularly polarized photons are provided at the output plane of the crystal (is Beta barium borate nonlinear crystal, (BBO) pumped by femtosecond optical pulses). They propagate through a birefringent material of a variable length l and then impinge on a 50/50 beamsplitter. Finally they are detected at the detectors D_A

and D_B . The coincidence-count rate R_c is measured by a coincidence device C . The beams might be filtered by the frequency filters F_A and F_B which can be placed in front of the detectors. Analyzers rotated by 45° with respect to the ordinary and extraordinary axes of the nonlinear crystal enable quantum interference between two paths to be observed; either a photon from beam 1 is detected by the detector D_A and a photon from beam 2 by the detector D_B , or vice versa. Including the effects of the beamsplitter and analyzers, the coincidence-count rate R_c can be determined as follows:

$$R_c(l) = \frac{1}{4} \int_{-\infty}^{\infty} dt_A \int_{-\infty}^{\infty} dt_B |A_{12,l}(t_A, t_B) - A_{21,l}(t_B, t_A)|^2 \dots (1)$$

The normalized coincidence-count rate R_n is then expressed in the form [6,4]:

$$R_n(l) = 1 - \rho(l) \dots (2)$$

Where

$$\rho(l) = \frac{1}{2R_0} \int_{-\infty}^{\infty} dt_A \int_{-\infty}^{\infty} dt_B \text{Re} [A_{12,l}(t_A, t_B) A_{21,l}^*(t_B, t_A)] \dots (3)$$

and

$$R_0 = \frac{1}{2} \int_{-\infty}^{\infty} dt_A \int_{-\infty}^{\infty} dt_B |A_{12,l}(t_A, t_B)|^2 \dots (4)$$

Where

$\rho(l)$ represent function of the length l of the birefringent material

R_0 represent normalization constant

Let us assume that the nonlinear crystal and the optical material in the path of the down-converted photons are both dispersive.

The wave vectors $k_p(\omega_{k_p})$, $k_1(\omega_{k_1})$, and $k_2(\omega_{k_2})$ of the beams in the nonlinear crystal can be expressed in the following form, when the effects of material dispersion up to the second order are included [8]:

$$k_j(\omega_{k_j}) = k_j^0 + \frac{1}{v_j} (\omega_{k_j} - \omega_j^0) + \frac{D_j}{4\pi} (\omega_{k_j} - \omega_j^0)^2, \quad j = 1, 2 \dots (5)$$

The inverse of group velocity $\frac{1}{v_j}$ and the second-order dispersion coefficient D_j are given by [7]

$$\frac{1}{v_j} = \left. \frac{dk_j}{d\omega_{k_j}} \right|_{\omega_{k_j} = \omega_j^0} \dots (6)$$

$$D_j = 2\pi \left. \frac{d^2 k_j}{d\omega_{k_j}^2} \right|_{\omega_{k_j} = \omega_j^0}, \quad j = 1, 2 \dots (7)$$

The symbol ω_j^0 denotes the central frequency of beam j . The wave vector k_j^0 is defined by the relation $k_j^0 = k_j(\omega_j^0)$. Similarly, the wave vectors $\tilde{k}_1(\omega_{k_1})$ and $\tilde{k}_2(\omega_{k_2})$ of the down-converted beams in a dispersive material outside the crystal can be expressed as

$$\tilde{k}_j(\omega_{k_j}) = \tilde{k}_j^0 + \frac{1}{\tilde{v}_j} (\omega_{k_j} - \omega_j^0) + \frac{\tilde{D}_j}{4\pi} (\omega_{k_j} - \omega_j^0)^2, \quad j = 1, 2 \dots (8)$$

where

$$\frac{1}{\tilde{v}_j} = \left. \frac{d\tilde{k}_j}{d\omega_{k_j}} \right|_{\omega_{k_j} = \omega_j^0} \dots (9)$$

$$\tilde{D}_j = 2\pi \left. \frac{d^2 \tilde{k}_j}{d\omega_{k_j}^2} \right|_{\omega_{k_j} = \omega_j^0}, \quad j = 1, 2 \dots (10)$$

and $\tilde{k}_j^0 = \tilde{k}_j(\omega_j^0)$.

Assuming, frequency- and wave-vector phase matching for the central frequencies $(\omega_p^0 = \omega_1^0 + \omega_2^0)$ and central wave vectors $(k_p^0 = k_1^0 + k_2^0)$, respectively. Considering an ultrashort pump pulse with a Gaussian profile: the

envelope $\xi_p^{(+)}(0, t)$ of the pump pulse at the output plane of the crystal then assumes the form [9]

$$\xi_p^{(+)}(0, t) = \xi_{p0} \exp\left\{ \frac{1 + ia}{\tau_D} t^2 \right\} \dots (11)$$

where ξ_{p0} is the amplitude, τ_D is the pulse duration, and the parameter a describes the chirp of the pulse.

The complex spectrum $\xi_p^{(+)}(z, \Omega_p)$ of the envelope $\xi_p^{(+)}(z, t)$ is defined by [9]:

$$\xi_p^{(+)}(z, \Omega_p) = \frac{1}{2\pi} \int_{-\infty}^{\infty} \xi_p^{(+)}(z, t) \exp(i\Omega_p t) dt \dots (12)$$

For a pulse of the form given in eq. (11) we obtain

$$\xi_p^{(+)}(0, \Omega_p) = \xi_{p0} \frac{\tau_D}{2\sqrt{\pi} \sqrt{1-a^2}} \exp\left\{ -\frac{\tau_D^2}{4(1+a^2)} (1-ia)\Omega_p^2 \right\} \dots (13)$$

where $\xi_p = \xi_{p0} \exp\left(\frac{-i \arctan(a)}{2}\right)$.

The quantities $\rho(l)$ and R_0 are then determined in accordance with their definitions in eqs. (2) and (3), respectively. The quantity $\rho(l)$ as a function of the length l of the birefringent material then takes the form ($\omega_1^0 = \omega_2^0$ is assumed).

$$\rho(l) = \frac{D_1 D_2}{4(1+a^2)} \left[\frac{1}{\sqrt{1+a^2}} \exp\left\{ \frac{D_1 D_2}{4\pi} \left(\frac{1}{\sqrt{1+a^2}} \right)^2 \right\} \right] \dots (14)$$

The functions $\bar{\beta}_j(z_1, z_2)$, $\bar{c}_j(z_1, z_2)$, and $\bar{y}_j(z_1, z_2)$ are expressed as follows:

$$\begin{aligned} \bar{\beta}_j(z_1, z_2) &= \frac{1}{a_j^2} \left[\frac{D_j D_k}{4\pi} \left(\frac{1}{\sqrt{1+a_j^2}} \right)^2 \right] \dots (15) \\ \bar{c}_j(z_1, z_2) &= \frac{1}{a_j^2} \left[\frac{D_j D_k}{4\pi} \left(\frac{1}{\sqrt{1+a_j^2}} \right)^2 \right] \dots \\ \bar{y}_j(z_1, z_2) &= \frac{1}{a_j^2} \left[\frac{D_j D_k}{4\pi} \left(\frac{1}{\sqrt{1+a_j^2}} \right)^2 \right] \dots \end{aligned}$$

Similarly, the normalization constant R_0 is given by the expression [10].

$$R_0 = \frac{\pi^2 C_0^2 |\xi_p^{(+)}|^2 \int_{-\infty}^{\infty} dt_1 \int_{-\infty}^{\infty} dt_2}{2\sqrt{1+a^2} \sqrt{1+a^2}} \exp\left[\frac{D_1 D_2}{4\pi} \left(\frac{1}{\sqrt{1+a^2}} \right)^2 \right] \dots (16)$$

Where

$$\begin{aligned} \bar{\beta}_j(z_1, z_2) &= \frac{1}{a_j^2} \left[\frac{D_j D_k}{4\pi} \left(\frac{1}{\sqrt{1+a_j^2}} \right)^2 \right] \dots (17) \\ \bar{c}_j(z_1, z_2) &= \frac{1}{a_j^2} \left[\frac{D_j D_k}{4\pi} \left(\frac{1}{\sqrt{1+a_j^2}} \right)^2 \right] \dots \\ \bar{y}_j(z_1, z_2) &= \frac{1}{a_j^2} \left[\frac{D_j D_k}{4\pi} \left(\frac{1}{\sqrt{1+a_j^2}} \right)^2 \right] \dots \end{aligned}$$

It is convenient to consider the pump-pulse characteristics at the output plane of the crystal, i.e., to use the parameters τ_D and a . They can be expressed in terms of the parameters τ_{Di} and a_i appropriate for the input plane of the crystal [10]:

$$a = \frac{1}{4(1+a^2)} \left[\frac{D_1 D_2}{4\pi} \left(\frac{1}{\sqrt{1+a^2}} \right)^2 \right] \dots (18)$$

The parameter b is a characteristic parameter of the pump pulse:

$$b = \frac{\tau_D^2}{4(1+a^2)} \dots (19)$$

Results and Dissociation

Second-order dispersion in an optical material (d_1 , d_2) through which down-converted photons propagate leads to asymmetry of the dip. The dip is particularly stretched to larger values of l in case $L=3\text{mm}$ (see Fig.(2)) as a consequence of the deformation and lengthening of the two-photon amplitude $A_{12,l}$ in a dispersive material. The higher is the difference (d_1-d_2) of the dispersion parameters, the higher is the asymmetry and the wider the dip; moreover, its minimum is shifted further to smaller values of l . Asymmetry of the dip is also observed when relatively narrow frequency filters are used though the narrowest filters remove it. Chirp decreases visibility but the shape of the dip remains unchanged. While fig. (2) b & c show that the interference pattern will be more asymmetry and deformed for long crystal ($L=5\text{mm}$) and higher difference of the dispersion parameter.

Asymmetry of the dip is caused by the second-order dispersion in an optical material through which down-converted photons propagation can be suppressed in two cases. In the first case, for a pump pulse of arbitrary duration, dispersion cancellation occurs when the magnitude of second-order dispersion in the path of the first photon (given by d_1l) equals that of the second photon (given by d_2l). This observation is immediate, when the pulse duration is sufficiently long (in the CW regime), dispersion cancellation occurs for arbitrary magnitudes of second-order dispersion (given by d_1l and d_2l) present in the paths of the down-converted photons. The gradual suppression of the asymmetry of the dip as the pump-pulse duration increases is shown in Fig. (3) c & d, which show the triangle shape of interference will be wider for long crystal.

Dispersion cancellation has its origin in the entanglement of the photons,

i.e., in the fact that the permitted values of the frequency ω_1 and the frequency ω_2 are governed by the relation $\delta(\omega_p - \omega_1 - \omega_2)$, where ω_p lies within the pump pulse spectrum. From fig.(4) we found that highest visibility occurs at chirp parameter $a_i=0$ and at birefringent material length $=5\text{mm}$ at pulse duration 9×10^{-13} .

Conclusions

The coincidence visibility decreases dramatically with increasing crystal length when using pulsed pump, reversing the state when used CW pump an especially with small aperture diameter ($\sim 0.25\text{mm}$) the visibility decrease slowly. Moreover, The effect of the pump beam diameter on the quantum interference pattern is shown to be negligible for a typical range of pump diameter values used. Second order dispersion of the pump beam in the non-linear crystal can result in occurrence of the local peak at the bottom of the interference dip.

References

- [1] Reinhard Erdmann, "Restoring dispersion cancellation for entangled photons produced by ultra short pulses" Physical Review A, Vol.62, P.53810 (2000).
- [2] Yoon-Ho Kim, " Measurement of the spectral properties of the two photon state generated via type II spontaneous parametric down conversion, Optics Letters " Vol. 30, No. 8 (2005).
- [3] Jan perina, Jr., Alexander V. sergienko, Bradley M. Jost, Bahaa E.A. Saleh, and marlin C. Teich, "Dispersion in femtosecond Entangled Two-Photon Interference", Phys.Rev., A, Vol.59, No. 3,(1999).
- [4] G. Di Giuseppe, L. Haiberger, and F. De Martini, "Quantum interference and in distinguishability with femtosecond pulses", Phys. Rev. A, Vol.56, No. 1, (1997).
- [5] N .Grate & H.Venghaus, "Fiber Optics Communication Device", Springer Verlag,(1998).

[6] Gunther Mahlke & Peter Gossing, "Fiber Optics Cables", Publicis MCD Corporate Publishing, (2001).

[7] D. S. Naik, C. G. Peterson, A. G. White., "Entanglement enhanced quantum cryptography fiber systems" University of Illinois, Urbana-Champaign, the European Community,(2002)

[8] Frenck Krausz, Ernst Wintner, "Ultra short light pulse" Lecture notes, Vienna University,(2001).

[9] Ivan Ordavo, " Free-Space Quantum Cryptography", Diploma Thesis , Department für Physik, (2006).

[10] Mete Atatüre, Alexander V. Sergienko, Bahaa E. A. Saleh, and Malvin C. Teich , "Entanglement in Cascaded-Crystal Parametric Down-Conversion "Physical Review letters" , Vol. 86, No. 18 (2001)

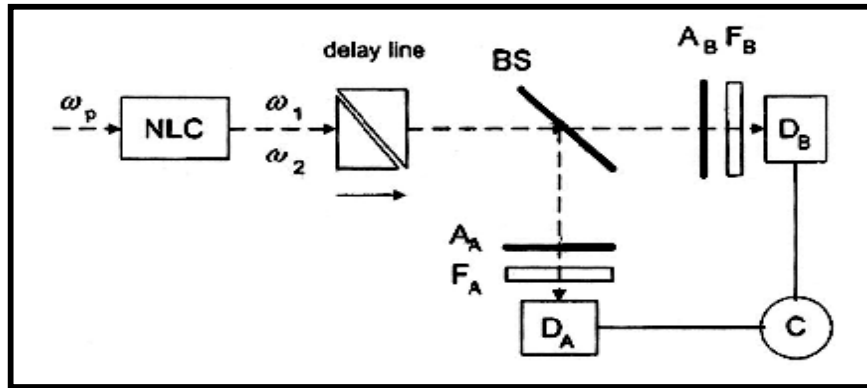


Figure (1) Sketch of the system under consideration: a pump pulse at the frequency ω_p generates down-converted photons at frequencies ω_1 and ω_2 in the nonlinear crystal[3]

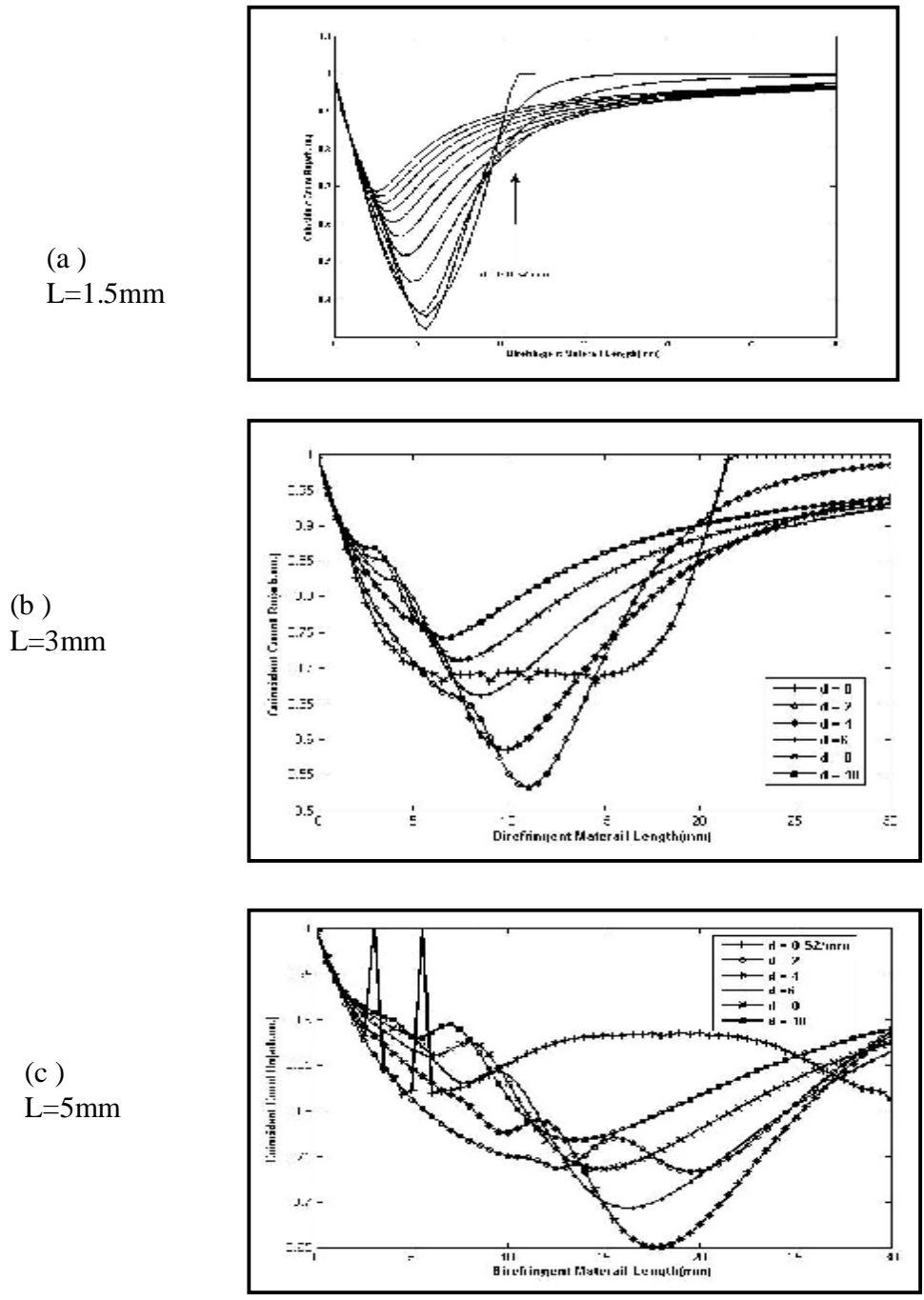


Figure.(2) coincident count rate $R_n(l)$ for different value of second order dispersion parameter (d) $L=(a-1.5mm, b-3mm, c-5mm), \tau_d=1.55 \times 10^{-13}, \sigma=50nm$ with small aperture diameter ($\sim 0.25mm$)

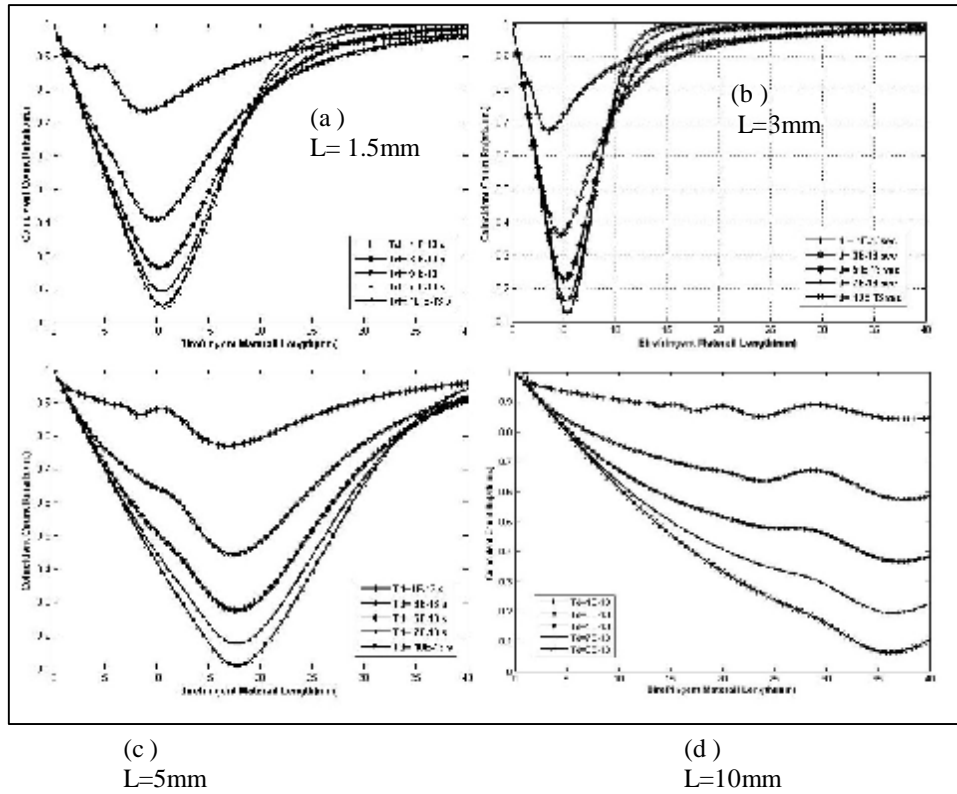
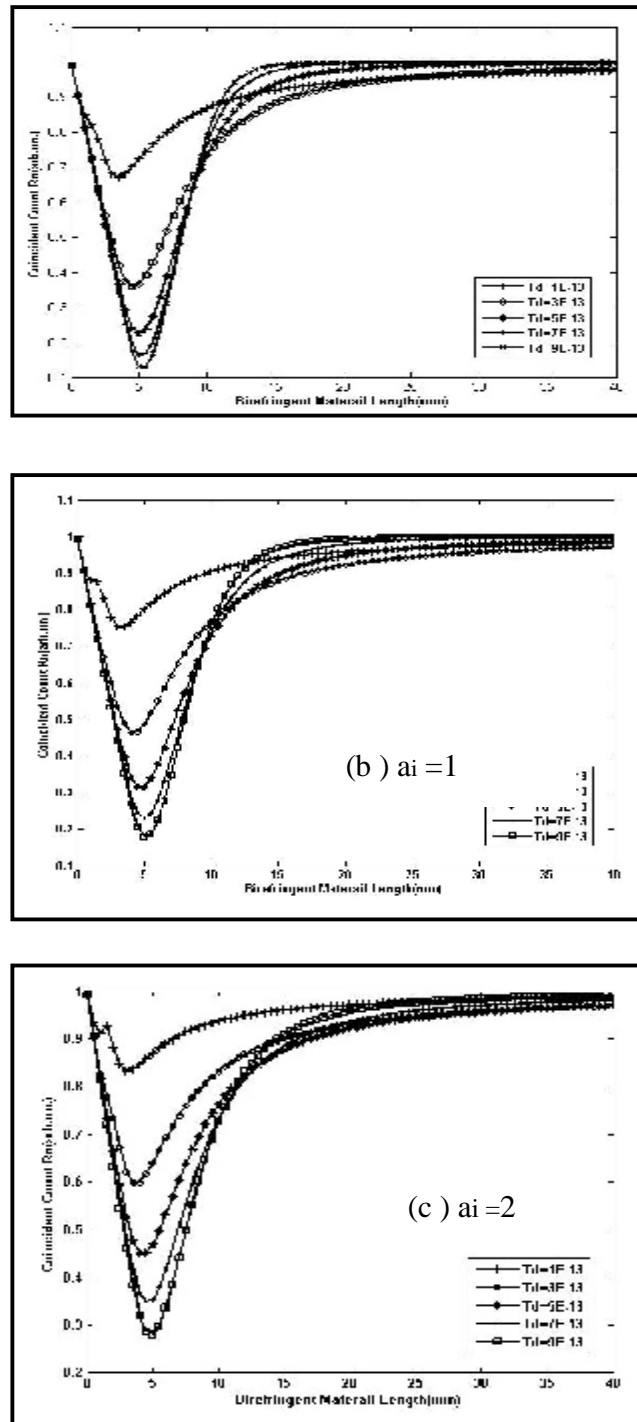


Figure.(3) Coincidence-count rate $R_n(l)$ shows a gradual suppression of dispersion effects(asymmetry)as the pump-pulse duration increases; for different crystal thickness $L(a=1.5mm,b=3mm, c=5mm, d=10mm)$ $S_1=S_2=50\text{ nm}$; values of the other parameters are zero



Figure(4) Coincident count rate as a function of (l) for different pulse duration t_p , for different chirp parameters value $a_i = (a-0, b-1, c-2)$